Electronic Supplementary Information for

Optical generation and electric control of pure spin photocurrent in ferroelectric Ruddlesden-Popper perovskite $(MA)_2Pb(SCN)_2I_2$ monolayer†

Yue Zhao,[ad] Xingchi Mu,[c] Gaoyang Gou,*[bd] Jian Zhou,*[c] Xiaoli Lu,[ad] and Yue Hao,*[ad]

[a] *China State Key Discipline Laboratory of Wide Band Gap Semiconductor Technology, Shaanxi Joint Key Laboratory of Graphene, Advanced Interdisciplinary Research Center for Flexible Electronics, School of Microelectronics, Xidian University, Xi'an 710071, China; E-mail: yhao@xidian.edu.cn*

[b] *Frontier Institute of Science and Technology, Xi'an Jiaotong University, Xi' an 710049, China. E-mail: gougaoyang@mail.xjtu.edu.cn*

[c] *Center for Alloy Innovation and Design, State Key Laboratory for Mechanical Behavior of Materials, Xi'an Jiaotong University, , Xi'an 710049, China. E-mail: jianzhou@xjtu.edu.cn*

[d] *Collaborative Innovation Center of Quantum Information of Shaanxi Province, Xidian University, Xi'an 710071, China*

Table S1: Comparison between the calculated (Cal) and experimentally measured (Exp[1]) crystallographic parameters for bulk $(MA)_2Pb(SCN)_2I_2$ in $Pmn2_1$ symmetry, d_{Pb} indicates the polar displacement of Pb cation relative to $Pb(SCN)_2I_4$ octahedral center.

FE bulk $(MA)_2Pb(SCN)_2I_2$						
Exp: a = 18.580 Å, b = 6.267 Å, c = 6.466 Å, d_{Pb} = 0.202 Å						
Cal: a = 17.849 Å, b = 6.178 Å, c = 6.398 Å, d_{Pb} = 0.374 Å						
	Exp			Cal		
Atom	x	y	z	x	y	z
Pb (2a)	0.50000	0.39288	0.23378	0.50000	0.37280	0.22410
I (2a)	0.50000	0.89281	0.27687	0.50000	0.86758	0.29457
I (2a)	0.50000	0.36268	-0.25772	0.50000	0.33813	-0.26116
S (4b)	0.34205	0.32704	0.22918	0.33470	0.31644	0.22633
C (4b)	0.31055	0.56112	0.26832	0.30834	0.56446	0.26784
C (4b)	0.35707	-0.14562	0.80520	0.36188	-0.15622	0.80944
N (4b)	0.28684	0.73142	0.29692	0.28881	0.74391	0.29686
N (4b)	0.33454	0.00682	0.65212	0.33271	-0.00206	0.65161
H (4b)	0.29860	0.08530	0.70240	0.28604	0.08255	0.70561
H (4b)	0.31960	-0.06180	0.53940	0.31799	-0.08284	0.51496
H (4b)	0.37130	0.09120	0.61970	0.37284	0.11081	0.61558
H (4b)	0.37630	-0.07170	0.92270	0.37064	-0.07151	0.95627
H (4b)	0.39320	-0.23720	0.74750	0.41466	-0.22228	0.75324
H (4b)	0.31640	-0.22980	0.84760	0.32112	-0.28525	0.83067

Table S2: Our calculated (Cal) energy gaps (E_g in eV) for Perovskite $(MA)_2Pb(SCN)_2I_2$ bulk and monolayer using the different α and μ parameter values. HSE+SOC calculations with $\alpha = 0.43$ and $\mu = 0.2$ can predict E_g closer to the experimental (Exp) results. The direct E_g of $(MA)_2Pb(SCN)_2I_2$ are provided in parentheses.

	Cal		Exp
	$\alpha = 0.3$, $\mu = 0$	$\alpha = 0.43$, $\mu = 0.2$	
bulk	2.29 (2.43)	2.15 (2.26)	2.04 (2.11)
mono	2.78 (2.86)	2.63 (2.68)	−−

Table S3: Predicted crystallographic parameters for 2D FE $(MA)_2Pb(SCN)_2I_2$ monolayer in $Pmc2_1$ symmetry.

FE monolayer $(MA)_2Pb(SCN)_2I_2$			
x = 35.00 Å, y = 9.05 Å, z = 8.09 Å, d_{Pb} = 0.382 Å			
Atom	x	y	z
Pb (2a)	0.00000	0.23910	0.85342
I (2a)	0.00000	0.45508	0.54644
I (2a)	0.00000	0.09107	0.20575
S (4c)	-0.08517	0.21377	0.87874
C (4c)	-0.09739	0.32902	0.73433
C (4c)	0.89544	0.81653	0.82168
N (4c)	0.89409	0.41380	0.63000
N (4c)	-0.08377	0.67441	0.81034
H (4c)	-0.08791	0.38260	0.42097
H (4c)	-0.09319	0.60684	0.71551
H (4c)	-0.05502	0.30827	0.29471
H (4c)	-0.09964	0.88066	0.71041
H (4c)	-0.09386	0.12331	0.42829

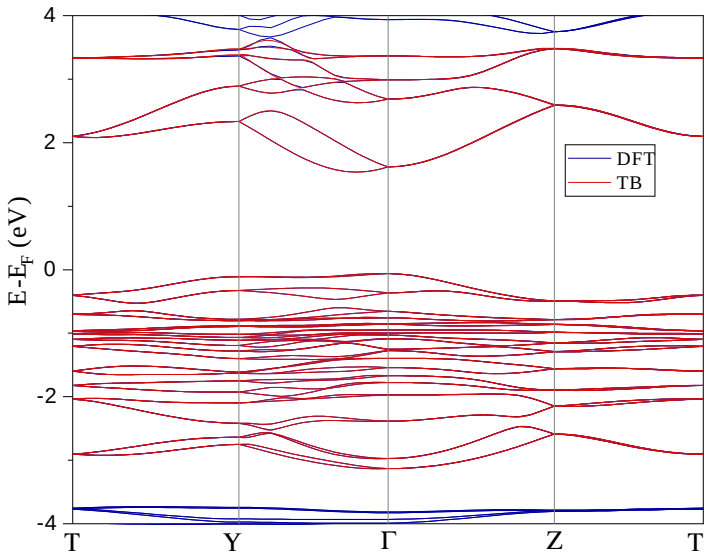

Figure S1: Comparison of band structure for $(MA)_2Pb(SCN)_2I_2$ monolayer predicted by DFT(PBE functional) and tight binding (TB) fitting performed using the Wannier90 package. SOC effect is included self-consistently. Owing to the underestimation of band gap from PBE functional, scissor operator is applied to correct PBE band gap to the target value predicted HSE06 hybrid functional.

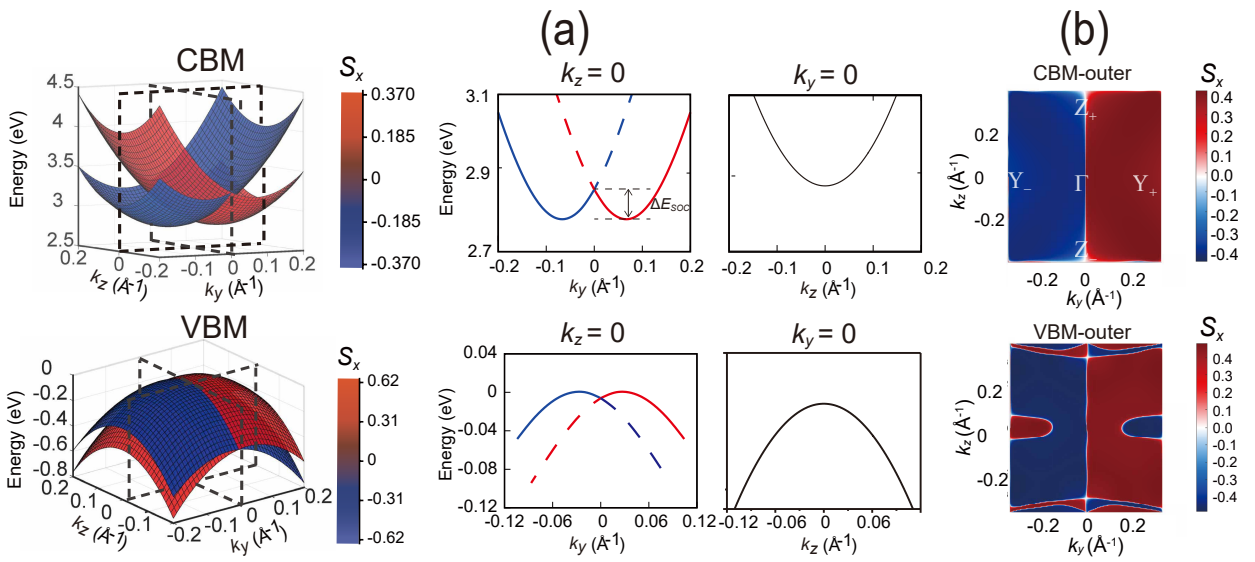

Figure S2: Spin-split band structure and spin texture obtained from $-P$ state of FE-$(MA)_2Pb(SCN)_2I_2$ monolayer. (a) 3D contour plots for spin-split top of the valence and bottom of conduction bands among 2D reciprocal space. The dispersion of spin-resolved and spin-degenerate energy bands along k_y and k_z directions are obtained, after projection 3D bands into $k_z = 0$ and $k_y = 0$ reciprocal planes, respectively. (b) Spin texture for outer valence and conduction band branches among 2D Brillouin zone of $(MA)_2Pb(SCN)_2I_2$ monolayer, predicted by TB Hamiltonian constructed using Wannier90 package. Compared with the results from Fig. 3 of main text, switching of in-plane ferroelectricity between $+/-P$ states of FE-$(MA)_2Pb(SCN)_2I_2$ monolayer can lead to the reversal of out-of-plane spin orientations.

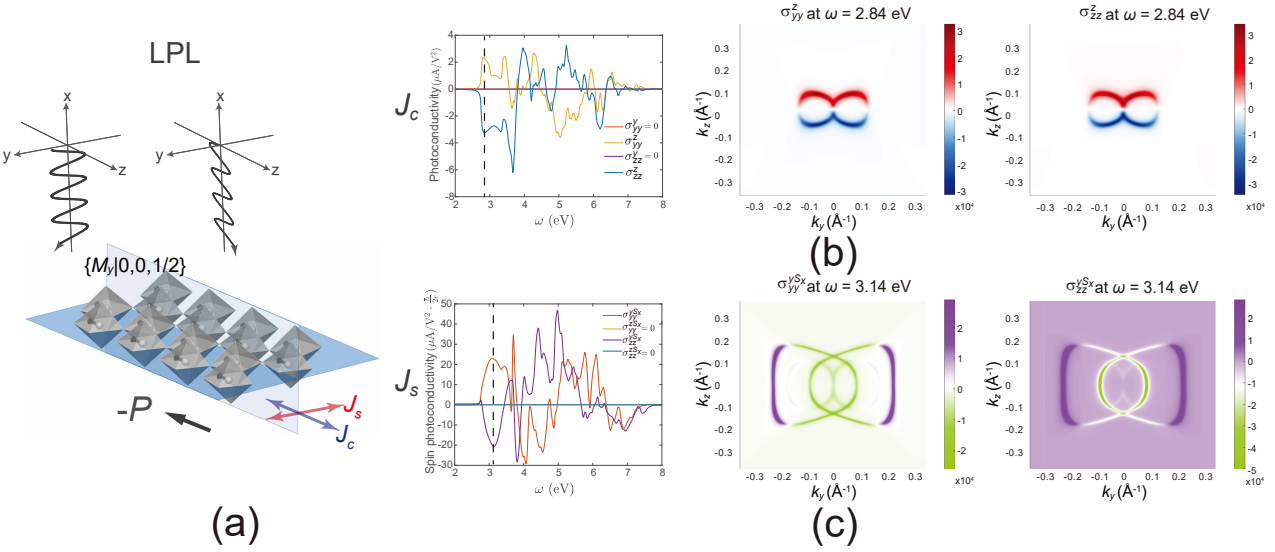

Figure S3: (a) Schematic diagram for generation of charge and spin photocurrent in $-P$ state of FE-$(MA)_2Pb(SCN)_2I_2$ monolayer, under the illumination of LPL propagating along x axis, polarized along y and z axes, respectively. The spatially separated pure spin and charge photocurrent (J_s and J_c) can be obtained along planar y and z axes, respectively. (b) Calculated J_C conductivity, and the distribution of non-zero conductivity components $\sigma^z_{yy}(k)$ and $\sigma^z_{zz}(k)$ among 2D reciprocal space of $(MA)_2Pb(SCN)_2I_2$ monolayer, under the incident LPL with photon energy $\omega = 2.84$ eV. It is noted the color bar in different scales are marked for $\sigma^z_{yy}(k)$ and $\sigma^z_{zz}(k)$ components. (c) Calculated J_S conductivity with out-of-plane spin component S_x, and the distributions of non-zero spin current conductivity components $\sigma^{yS_x}_{yy}(k)$ and $\sigma^{yS_x}_{zz}(k)$ among 2D reciprocal space, under the incident LPL with photon energy $\omega = 3.14$ eV. It is clearly shown that LPL induced J_C and J_S will have their current directions reversed, when in-plane polarization is switched from $+P$ to $-P$ state of FE-$(MA)_2Pb(SCN)_2I_2$ monolayer.

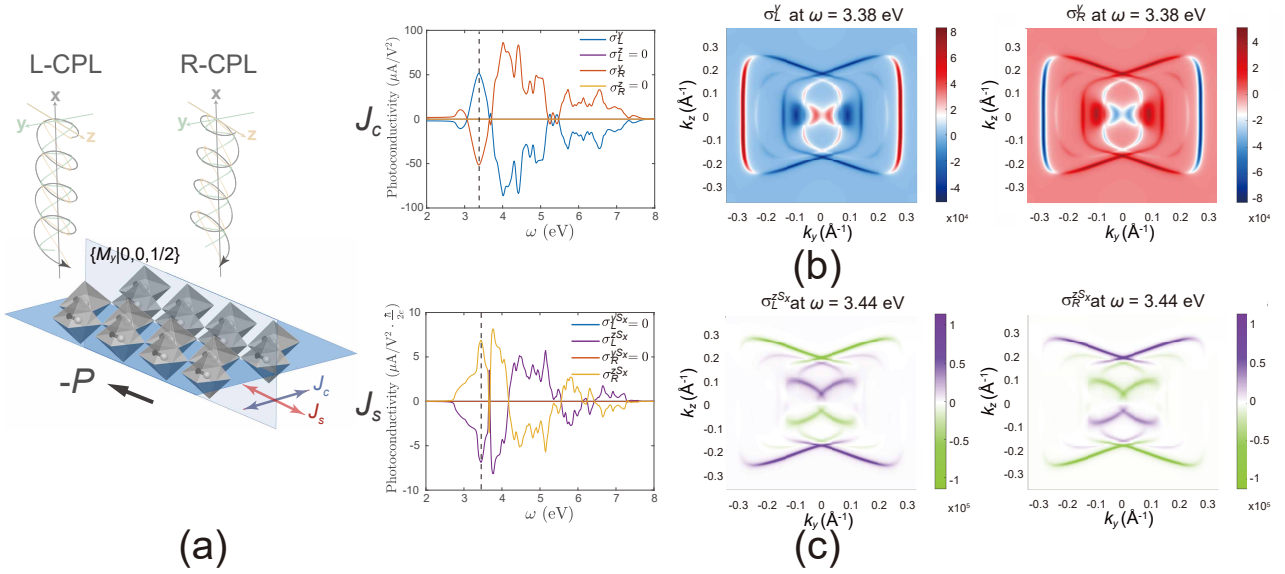

Figure S4: (a) Schematic diagram for generation of charge and spin photocurrent in $-P$ state of FE-$(MA)_2Pb(SCN)_2I_2$ monolayer, under the illumination of L-CPL and R-CPL propagating along x axis, respectively. The spatially separated pure charge and spin photocurrent (J_c and J_s) can be obtained along planar y and z axes, respectively. (b) Calculated J_C, and the distribution of non-zero conductivity components $\sigma_L^y(k)$ and $\sigma_R^y(k)$ among 2D reciprocal space of $(MA)_2Pb(SCN)_2I_2$ monolayer, under the incident L-CPL and R-CPL with photon energy $\omega = 3.38$ eV, respectively. (c) Calculated J_S conductivity with out-of-plane spin component S_x, and the distributions of non-zero spin current conductivity components $\sigma_L^{zS_x}(k)$ and $\sigma_R^{zS_x}(k)$ among 2D reciprocal space, under the incident L-CPL and R-CPL with photon energy $\omega = 3.44$ eV, respectively. It is clearly shown that CPL induced J_C and J_S will have their current directions reversed, when in-plane polarization is switched from $+P$ to $-P$ state of FE-$(MA)_2Pb(SCN)_2I_2$ monolayer.

References

[1] Z. Xiao, W. Meng, B. Saparov, H.-S. Duan, C. Wang, C. Feng, W. Liao, W. Ke, D. Zhao, J. Wang *et al.*, *J. Phy. Chem. Lett.*, 2016, **7**, 1213–1218.